Combining antibiotics with antivirulence compounds can have synergistic effects and reverse selection for antibiotic resistance in *Pseudomonas aeruginosa*

Chiara Rezzoagli[1,2,*], Martina Archetti[1,2,*], Ingrid Mignot[1], Michael Baumgartner[3], Rolf Kümmerli[1,2]

[1]Department of Quantitative Biomedicine, University of Zurich, Zurich, Switzerland

[2]Department of Plant and Microbial Biology, University of Zurich, Zurich, Switzerland

[3] Institute for Integrative Biology, Department of Environmental Systems Science, ETH Zurich, Zurich, Switzerland

[*] contributed equally to this work.

Short title: Antibiotic-antivirulence combination therapy against bacterial pathogens

Corresponding author: Rolf Kümmerli, Department of Quantitative Biomedicine, University of Zurich, Winterthurerstrasse 190, 8057 Zurich, Switzerland.

Email: rolf.kuemmerli@uzh.ch / Phone: +41 44 635 48 01.

Abstract

Antibiotics are losing efficacy due to the rapid evolution and spread of resistance. Treatments targeting bacterial virulence factors have been considered as alternatives because they target virulence instead of pathogen viability, and should therefore exert weaker selection for resistance than conventional antibiotics. However, antivirulence treatments rarely clear infections, which compromises their clinical applications. Here, we explore the potential of combining antivirulence drugs with antibiotics against the opportunistic human pathogen *Pseudomonas aeruginosa*. We combined two antivirulence compounds (gallium, a siderophore-quencher, and furanone C-30, a quorum sensing-inhibitor) together with four clinically relevant antibiotics (ciprofloxacin, colistin, meropenem, tobramycin) in 9x9 drug concentration matrices. We found that drug-interaction patterns were concentration dependent, with promising levels of synergies occurring at intermediate drug concentrations for certain drug pairs. We then tested whether antivirulence compounds are potent adjuvants, especially when treating antibiotic resistant clones. We found that the addition of antivirulence compounds to antibiotics could restore growth inhibition for most antibiotic resistant clones, and even abrogate or reverse selection for resistance in five drug combination cases. Molecular analyses suggest that selection against resistant clones occurs when resistance mechanisms involve restoration of protein synthesis, but not when efflux pumps are upregulated. Altogether, our work provides a first systematic analysis of antivirulence-antibiotic combinatorial treatments and suggests that such combinations have a high potential to be both effective in treating infections and in limiting the spread of antibiotic resistance.

Introduction

Scientists together with the World Health Organization (WHO) forecast that the rapid evolution and spread of antibiotic resistant bacteria will lead to a world-wide medical crisis [1–3]. Already today, the effective treatment of an increasing number of infectious diseases has become difficult in many cases [4,5]. To avert the crisis, novel innovative approaches that are both effective against pathogens and robust to the emergence and spread of resistance are urgently needed [6,7]. One such approach involves the use of compounds that disarm rather than kill bacteria. These so-called 'antivirulence' treatments should exert weaker selection for resistance compared to classical antibiotics because they simply disable virulence factors but are not supposed to affect pathogen viability [8–10]. However, a downside of antivirulence approaches is that the infection will not necessarily be cleared. This could be particularly problematic for immuno-compromised patients (AIDS, cancer, cystic fibrosis and intensive-care unit patients), whose immune system is conceivably too weak to clear even disarmed pathogens.

One way to circumvent this problem is to combine antivirulence compounds with antibiotics to benefit from both virulence suppression and effective pathogen removal [6,11]. While a few studies have already considered such combinatorial treatments [12–18], we currently have no comprehensive understanding of how different types of antibiotics and antivirulence drugs interact, whether interactions are predominantly synergistic or antagonistic, and how combinatorial treatments affect growth and the spread of antibiotic resistant strains. Such knowledge is, however, essential if such therapies are supposed to make their way into the clinics, as drug interactions and their effects on antibiotic resistance evolution will determine both the efficacy and

70 sustainability of treatments. Here, we tackle these open issues by combining four
71 different classes of antibiotics with two antivirulence compounds as treatments against
72 the opportunistic human pathogen *Pseudomonas aeruginosa*, to test the nature of drug
73 interactions, and the usefulness of antivirulence compounds as adjuvants to combat
74 antibiotic sensitive and resistant strains.
75
76 *P. aeruginosa* is one of the ESKAPE pathogens with multi-drug resistant strains
77 spreading worldwide and infections becoming increasingly difficult to treat [19,20]. In
78 addition to its clinical relevance, *P. aeruginosa* has become a model system for
79 antivirulence research [21]. Several antivirulence compounds targeting either the
80 species' quorum sensing (QS) [22–24] or siderophore-mediated iron uptake systems
81 [25–28] have been proposed. While QS is a cell-to-cell communication system that
82 controls the expression of multiple virulence factors including exo-proteases,
83 biosurfactants and toxins, siderophores are secondary metabolites important for the
84 scavenging of iron from host tissue. For our experiments, we chose antivirulence
85 compounds that target these two different virulence mechanisms: furanone C-30, an
86 inhibitor of the LasR QS-system [12,22], and gallium, targeting the iron-scavenging
87 pyoverdine and iron-metabolism [25,27,29–33].
88
89 Furanone C-30 is a synthetic, brominated furanone, which includes the same lactone
90 ring present in the acylhomoserine lactones (AHL) QS molecules of *P. aeruginosa* [34].
91 As a consequence, it can disrupt QS-based communication by antagonistically
92 competing with the AHLs molecules for binding to the main QS (LasR) receptor in a
93 concentration dependent manner [12,35]. Gallium is an iron mimic whose ionic radius
94 and coordination chemistry is comparable to ferric iron, although its redox properties

are different. Specifically, gallium cannot be reduced and thereby irreversibly binds to siderophores and hinders siderophore-mediated iron uptake [25,27]. Pyoverdine is controlled in complex ways involving information on cell density and feedbacks from iron uptake rates [36,37]. Gallium interferes with these regulatory circuits, whereby cells intermittently upregulate pyoverdine production at low gallium concentrations to compensate for the increased level of iron limitation, and down-regulate pyoverdine production at higher gallium concentrations because iron uptake via this pathway is unsuccessful [27]. Importantly, gallium drastically reduces pyoverdine availability at the population level in a concentration-dependent manner [25,38].

We combined the two antivirulence compounds with four clinically relevant antibiotics (ciprofloxacin, colistin, meropenem, and tobramycin), which are widely used against *P. aeruginosa* [39]. In a first step, we measured treatment effects on bacterial growth and virulence factor production for all eight drug combinations for 81 concentration combinations each. In a second step, we applied the Bliss independence model to calculate the degree of synergy or antagonism to obtain comprehensive interaction maps for all combinations both for growth and virulence factor production. Next, we selected for antibiotic resistant clones and tested whether the addition of antivirulence compounds as adjuvants restores growth inhibition and affects selection for antibiotic resistance. Finally, we sequenced the genomes of the evolved antibiotic resistant clones to understand the genetic basis that drive the observed effects on pathogen growth and selection for or against antibiotic resistance.

118 ## Results

119 **PAO1 dose-response curves to antibiotics and antivirulence compounds**

120 In a first experiment, we determined the dose-response curve of PAO1 to each of the
121 four antibiotics (Fig 1) and the two anti-virulence compounds (Fig 2) in our
122 experimental media. We found that the dose-response curves for antibiotics followed
123 sigmoid functions (Fig 1), characterised by (i) a low antibiotic concentration range that
124 did not inhibit bacterial growth, (ii) an intermediate antibiotic concentration range that
125 significantly reduced bacterial growth, and (iii) a high antibiotic concentration range
126 that completely stalled bacterial growth. Since antibiotics curbed growth, they
127 congruently also reduced the availability of virulence factors at the population level (S1
128 Fig).

129

130 Similarly shaped dose-response curves for growth (Fig 2A) and virulence factor
131 production (Fig 2B) were obtained for gallium (quenching pyoverdine) and furanone C-
132 30 (inhibiting protease production) in the respective media where the two virulence
133 factors are important for growth. Under such conditions, the reduced availability of
134 virulence factors immediately feeds back on growth by inducing iron starvation
135 (gallium) or the inability to degrade proteins (furanone). Crucially, the dose-response
136 curves for growth shifted to the right (extending phase (i)) when we repeated the
137 experiment in media, where the virulence factors are not needed for growth (i.e. iron-
138 rich media for pyoverdine, and protein digest media for proteases). This shows that
139 there is a window of concentrations where growth inhibition is caused by virulence

140 factor quenching alone. Conversely, high concentrations of antivirulence compounds
141 seem to have additional off-target effects reducing growth.
142
143 **Interaction maps of antibiotic-antivirulence drug combinations**
144 *General patterns*. From the dose-response curves, we chose 9 concentrations for each
145 drug to cover the entire trajectory, from no to intermediate to high growth inhibition. We
146 then combined antibiotics with antivirulence compounds in a 9x9 concentration matrix
147 and measured the dose-response curve for every single drug combination for both
148 growth and virulence factor production (Fig 3). At the qualitative level, independent
149 drug effects would cause a symmetrical downshift of the dose-response curve with
150 higher antivirulence compound concentrations supplemented. We indeed noticed
151 symmetrical downshifts for many dose-response curves (Fig 3), but there were also
152 clear cases of non-symmetrical shifts, indicating synergy or antagonism between
153 drugs. We then used the Bliss model, representing the adequate model for drugs with
154 independent modes of actions, to quantify these effects. We found patterns of synergy
155 and antagonism for both growth and virulence factor inhibition across the concentration
156 matrices for all drug combinations (Fig 4), with many of these interactions being
157 significant (S2 Fig).
158
159 *Gallium-antibiotic combinations*. Gallium combined with ciprofloxacin or colistin had
160 mostly independent effects on bacterial growth (i.e. weak or no synergy/antagonism)
161 (Fig 4A+B). With regard to the inhibition of pyoverdine production, both drug
162 combinations showed significant levels of synergy at intermediate drug concentrations
163 (Fig 4E+F, S2 Fig). For gallium-meropenem combinations, we observed mostly
164 independent interactions for growth and pyoverdine inhibition, with small hotspots of

165 antagonism (for growth) and synergy (for siderophore inhibition) existing at
166 intermediate drug concentrations (Fig 4C+G). Finally, for gallium-tobramycin
167 combinations there were relatively strong significant synergistic interactions for both
168 growth and pyoverdine inhibition at intermediate drug concentrations (Fig 4D+H, S2
169 Fig). Interestingly, we observed synergy with regard to pyoverdine inhibition for all drug
170 combinations, indicating that the combination of low cell density induced by the
171 antibiotics and gallium-mediated pyoverdine quenching is a successful strategy to
172 repress this virulence factor.
173
174 *Furanone-antibiotic combinations*. For furanone-ciprofloxacin combinations, we found
175 relatively strong significant antagonistic interactions with regard to growth inhibition
176 (Fig 4I), whereas effects on protease inhibition were mostly independent (Fig 4M). In
177 contrast, for furanone-colistin combinations we observed strong and significant
178 synergistic drug interactions especially for intermediate and higher concentrations of
179 the antivirulence compound for growth and protease inhibition (Fig 4J+N, S2 Fig).
180 Furanone-meropenem, on the other hand, interacted mostly antagonistically with
181 regard to growth and protease inhibition (Fig 4K+O). Conversely, for furanone-
182 tobramycin combinations there were pervasive significant patterns of synergy across
183 the entire drug combination range for growth and virulence factor inhibition (Fig 4L+P,
184 S2 Fig).
185
186 *Do the degrees of synergy for growth and virulence factor inhibition correlate?* As the
187 combination treatments affect both growth and virulence factor production, we
188 examined whether the degrees of synergy correlate between the two traits (S3 Fig).
189 For gallium-antibiotic combinations, we found no correlations for ciprofloxacin and

190 meropenem, but positive associations for colistin and tobramycin (Pearson correlation
191 coefficient; ciprofloxacin: $r = 0.09$, $t_{79} = 0.85$, $p = 0.394$; colistin: $r = 0.69$, $t_{79} = 8.51$, p
192 < 0.001; meropenem: $r = 0.17$, $t_{79} = 1.53$, $p = 0.130$; tobramycin: $r = 0.58$, $t_{79} = 6.39$, p
193 < 0.001). For furanone-antibiotic combinations, there were strong positive correlations
194 between the levels of synergy for the two traits for all drug combinations (ciprofloxacin:
195 $r = 0.34$, $t_{79} = 3.22$, $p = 0.002$; colistin: $r = 0.96$, $t_{79} = 32.50$, $p < 0.001$; meropenem: $r =$
196 0.87, $t_{79} = 15.48$, $p < 0.001$; tobramycin: $r = 0.75$, $t_{79} = 10.16$, $p < 0.001$).
197

198 **Antibiotic resistance can lead to collateral sensitivity and cross-resistance to**
199 **antivirulence compounds**

200 In a next step, we asked whether antivirulence compounds could be used as adjuvants
201 to suppress the growth of antibiotic resistant clones. To address this question, we first
202 experimentally selected, isolated, and analyzed antibiotic resistant clones (AtbR). We
203 aimed for one clone per antibiotic and medium. In the end, we examined seven clones,
204 as only one selection line survived the ciprofloxacin selection regime (see methods for
205 details). We then assessed the dose-response curve of these clones for the respective
206 antibiotics to confirm and quantify their level of resistance (S4 Fig). We further
207 established the dose-response curves of all AtbR clones for the two antivirulence
208 compounds to test for collateral sensitivity and cross-resistance. Here, we compared
209 the IC50 (half maximal inhibitory concentration) values between the AtbR and wildtype
210 strain (Fig S5), and found evidence for weak but significant collateral sensitivity
211 between colistin and gallium and relatively strong collateral sensitivity between
212 tobramycin and furanone. Conversely, we found that resistance to ciprofloxacin,

213 colistin and also to some extent to meropenem can confer cross-resistance to furanone
214 (all statistical analyses are shown in S5 Fig).
215
216 Based on these experiments, we picked two concentrations for gallium (low: 1.56 μM;
217 intermediate: 6.25 μM) and furanone (low: 6.3 μM; intermediate: 22.8 μM) as adjuvants
218 in combination with antibiotics to test whether antivirulence compounds can restore
219 growth inhibition of and alter selection for AtbR clones.
220

221 **Antivirulence compounds as adjuvants can restore growth inhibition of**
222 **antibiotic resistant strains**

223 In a first set of experiments, we subjected all AtbR clones and the antibiotic-sensitive
224 wildtype to antivirulence treatments alone and to combination treatments with
225 antibiotics (Fig 5). For gallium, we observed that the wildtype and AtbR clones
226 responded almost identically to the antivirulence compounds in the absence of
227 antibiotics, showing that AtbR clones are still sensitive to gallium (Fig 5A). When
228 treated with antibiotics, we observed that the addition of anti-virulence compounds
229 consistently reduced growth of all AtbR clones (Fig 5A). The level of synergy between
230 drugs is similar for wildtype and AtbR clones, with the effects being close to zero
231 (varying between weak antagonism and weak synergy) in most cases. Altogether,
232 these findings indicate that gallium acts independently to all the tested antibiotics and
233 is still able induce iron starvation and thus reduce growth in AtbR clones. Important to
234 note is that gallium has a stronger growth inhibitory effect in this experiment compared

235 to the dose-response curve analysis (S5 Fig, collected after 48 hours), because this
236 experiment run for 24 hours only.
237
238 For furanone, the patterns were more diverse (Fig 5B). There were two cases of full
239 cross-resistance (ciprofloxacin and meropenem), where the addition of furanone no
240 longer had any effect on bacterial growth. In these cases, we observed a change from
241 weak drug synergy (for the wildtype) to strong drug antagonism (for the AtbR clones).
242 In contrast, we found a strong shift from weak antagonism (for the wildtype) to strong
243 drug synergy (for the AtbR clone) when furanone was combined with colistin. In this
244 case, furanone re-potentiated the antibiotic. Note that we initially also observed a
245 certain level of cross-resistance for this drug combination (S5 Fig), however only at
246 much higher furanone concentrations than those used here. Finally, the pattern
247 between tobramycin and furanone was driven by collateral sensitivity, where the
248 addition of furanone to the AtbR clone completely restored growth inhibition.
249
250 **Antivirulence as adjuvants can abrogate or reverse selection for antibiotic**
251 **resistance**
252 We then investigated whether antivirulence compounds alone or in combination with
253 antibiotics can influence the spread of AtbR clones in mixed populations with
254 susceptible wildtype cells (Fig 6). First, we competed the AtbR clones against the
255 susceptible wildtype in the absence of any treatment and observed that AtbR clones
256 consistently lost the competitions (one sample t-tests, $-13.50 \leq t_{15\text{-}26} \leq -2.62$, $p \leq 0.050$
257 for all comparisons). This confirms that antibiotic resistance is costly and is selected
258 against in the absence of treatment. We then added the antivirulence drug alone using
259 the same concentrations as for the monoculture experiments (Fig 5). We found that

260 the AtbR clones did not experience a selective advantage in 14 out 16 cases, with the
261 exception being one colistin resistant clone that slightly increased in frequency (Fig 6).
262 This analysis shows that the cost of AtbR resistance is largely maintained in the
263 presence of antivirulence compounds. Next, we exposed the mixed cultures to the
264 antibiotics alone and observed that, as expected, AtbR clones always experienced a
265 significant fitness advantage under treatment (one sample t-test, $4.54 \leq t_{19\text{-}26} \leq 13.41$,
266 $p < 0.001$ for all combinations).
267
268 When combining antivirulence compounds with antibiotics, three different relative
269 fitness patterns emerged for AtbR clones. In three cases (colistin-gallium,
270 ciprofloxacin-furanone and meropenem-furanone), AtbR clones experienced large
271 fitness advantages and were selectively favored regardless of whether the
272 antivirulence compound was present or not. In four cases (ciprofloxacin-gallium,
273 meropenem-gallium, tobramycin-gallium, colistin-furanone), the addition of
274 antivirulence compounds gradually reduced the relative fitness of the AtbR clones,
275 whereby in two cases (meropenem-gallium, tobramycin-gallium) the selective
276 advantage of AtbR clones was completely abrogated. Finally, in one case (tobramycin-
277 furanon) selection for AtbR clones was even reversed and AtbR clones lost the
278 competition.
279
280 **Drug synergy does not predict selection against antibiotic resistance**
281 We examined whether drug interactions, ranging from antagonism to synergy for both
282 AtbR clones and the wildtype (Fig 5) correlate with their relative fitness in competition
283 under combination treatments. However, we found no support for such associations
284 (S6 Fig, ANOVA, AtbR: $F_{1,65} = 0.88$, $p = 0.353$; WT: $F_{1,65} = 1.85$, $p = 0.179$, but instead

285 observed that variation in fitness patterns was explained by specific drug combinations
286 (antivirulence-antibiotic interaction, AtbR: $F_{3,65} = 37.45$, $p < 0.001$, WT: $F_{3,65} = 14.50$, p
287 < 0.001).
288

289 **Genetic basis of experimentally evolved antibiotic resistance**

290 The whole-genome sequencing of the experimentally evolved AtbR clones revealed a
291 small number of SNPs and INDELs, which are known to be associated with resistance
292 to the respective antibiotics (Table 1). The AtbR clone resistant to ciprofloxacin had
293 mutations in *gyrB*, a gene encoding the DNA gyrase subunit B, the direct target of the
294 antibiotic [40]. In addition, we identified an 18-bp deletion in the *mexR* gene, encoding
295 a multidrug efflux pump repressor [41]. The two AtbR clones resistant to colistin had
296 different mutations in the same target gene *phoQ* (a non-synonymous SNP in one
297 clone versus a 1-bp insertion in addition to a non-synonymous SNP in the other clone).
298 PhoQ is a regulator of the LPS modification operon and mutations in this gene
299 represent the first step in the development of high-level colistin resistance [42]. One
300 AtbR clone resistant to meropenem had a non-synonymous SNP in the coding
301 sequence of *mpl.* This gene encodes a murein tripeptide ligase, which contributes to
302 the overexpression of the beta-lactamase precursor gene *ampC* [43]. The other AtbR
303 clone resistant to meropenem had mutations in three different genes, which can all be
304 linked to antibiotic resistance mechanisms: we found (i) one non-synonymous SNP in
305 *parR*, which encodes a two component response regulator involved in several
306 resistance mechanisms, including drug efflux, porin loss and LPS modification [44]; (ii)
307 7 mutations in the *PA1874* gene, which encodes an efflux pump [45]; (iii) one non-
308 synonymous SNP in *nalD*, encoding the transcriptional regulator NalD, which regulates
309 the expression of drug-efflux systems [46,47]. Both AtbR clones resistant to tobramycin

310 had non-synonymous SNPs in *fusA1*. This gene encodes the elongation factor G, a
311 key component of the translational machinery. Although aminoglycosides do not
312 directly bind to the elongation factor G and the complete resistance mechanisms is still
313 unknown, mutations in *fusA1* are associated with high resistance to tobramycin and
314 are often found in clinical isolates [48,49].
315

316 ## Discussion

317 In this study, we systematically explored the effects of combining antibiotics with
318 antivirulence compounds as a potentially promising strategy to fight susceptible and
319 antibiotic resistant opportunistic human pathogens. Specifically, we combined four
320 different antibiotics (ciprofloxacin, colistin, meropenem, tobramycin) with two
321 antivirulence compounds (gallium targeting siderophore-mediated iron uptake and
322 furanone C-30 targeting the quorum sensing communication system) in 9x9 drug
323 interaction matrices against the bacterium *P. aeruginosa* as a model pathogen. Our
324 heat maps reveal drug-combination specific interaction patterns. While colistin and
325 tobramycin primarily interacted synergistically with the antivirulence compounds,
326 independent and antagonistic interactions occurred for ciprofloxacin and meropenem
327 in combination with the antivirulence compounds (Fig 3+4). We then used antivirulence
328 compounds as adjuvants and observed that they can restore growth inhibition of
329 antibiotic resistant clones in six out of eight cases (Fig 5). Finally, we performed
330 competition assays between antibiotic resistant and susceptible strains under single
331 and combinatorial drug treatments and found that antivirulence compounds can reduce

332 (two cases), abrogate (two cases) or even reverse (one case) selection for antibiotic
333 resistance (Fig 6).
334
335 Our results identify antibiotic-antivirulence combinations as a potentially powerful tool
336 to efficiently treat infections of troublesome nosocomial pathogens such as *P.*
337 *aeruginosa*. From the eight combinations analyzed, tobramycin-antivirulence
338 combinations emerged as the top candidate treatments because: (i) drugs interacted
339 synergistically both with regard to growth and virulence factor inhibition; (ii) the
340 antivirulence compounds restored growth inhibition of antibiotic resistant clones, and
341 even re-potentiated tobramycin in the case of furanone; and (iii) antivirulence
342 compounds either abrogated (for gallium) or even reversed (for furanone) selection for
343 tobramycin resistance, due to collateral sensitivity in the latter case. Meropenem-
344 gallium emerged as an additional promising combination, as this combination also
345 restored growth inhibition of the antibiotic resistant clone and abrogated its selective
346 advantage, despite this drug combination showing slight but significant antagonistic
347 effects.
348
349 Drug synergy is desirable from a clinical perspective because it allows to use lower
350 drug concentrations, thereby minimizing side effects while maintaining treatment
351 efficacy [50,51]. In this context, a number of studies have examined combinations of
352 antibiotics and antivirulence compounds targeting various virulence factors including
353 quorum sensing, iron uptake, and biofilm formation in *P. aeruginosa* [12,13,15–
354 18,23,52,53]. While some of these studies have used a few specific concentration
355 combinations to qualitatively assess synergy, we here present comprehensive
356 quantitative interaction maps for these two classes of drugs. A key insight of these

interaction maps is that specific drug combinations cannot simply be classified as either synergistic or antagonistic. Instead, drug interactions are concentration dependent with most parts of the interaction maps being characterized by independent effects interspersed with hotspots of synergy or antagonism (Fig 4, S2 Fig). The strongest effects of synergy and antagonism are often observed at intermediate drug concentrations, which is, in the case of synergy, ideal for developing combinatorial therapies that maximize treatment efficacy while minimizing toxicity for the patient. A crucial next step would be to test whether the same type of drug interactions can be recovered in animal host models.

While drug antagonism is considered undesirable from a clinical perspective, work on antibiotic combination therapies has revealed that antagonistic interactions can inhibit the spread of antibiotic resistance [54–56]. The reason behind this phenomenon is that when two drugs antagonize each other, becoming resistant to one drug will remove the antagonistic effect on the second drug, such that the combination treatment will be more effective against the resistant clones [54]. We suspected that such effects might also occur for antagonistic antibiotic-antivirulence treatments, and indeed the meropenem-gallium combination discussed above matches this pattern. However, when comparing across all the eight combinations, we found no evidence that the selection for or against antibiotic resistant clones correlates with the type of drug interaction (S6 Fig). A possible explanation for the overall absence of an association is that the antagonism between antibiotics and antivirulence compounds was quite moderate. In contrast, previous work used an extreme case of antagonism, where the

380 effect of one drug was almost completely suppressed in the presence of the second
381 drug [54,56].
382
383 We propose that it is rather the underlying molecular mechanism and not the direction
384 of drug interaction that determines whether selection for antibiotic resistance is
385 compromised or maintained. For instance, any resistance mechanism that reduces
386 antibiotic entry or increases its efflux could conceivably confer cross-resistance to
387 antivirulence compounds, which should in turn maintain or even potentiate and not
388 reverse selection for antibiotic resistance. This phenomenon could explain the patterns
389 observed for furanone in combination with ciprofloxacin and meropenem, where in both
390 cases our sequencing analysis revealed mutations in genes regulating efflux pumps
391 (Table 1). Since furanone needs to enter the cells to become active, these mutations,
392 known to confer resistance to antibiotics [41,42,45], likely also confer resistance to
393 furanone [57]. In contrast, efflux pumps upregulation cannot work as a cross-resistance
394 mechanism against gallium, which binds to secreted pyoverdine and thus acts outside
395 the cell [38].
396
397 Alternatively, competitive interactions between resistant and sensitive pathogens over
398 common resources could compromise the spread of drug resistance, as shown for
399 malaria parasites [58]. In our case, it is plausible to assume that antibiotic resistant
400 clones are healthier than susceptible cells and might therefore produce higher amounts
401 of pyoverdine and proteases under antivirulence treatment. Since these virulence
402 factors are secreted and shared between cells, antibiotic resistant clones take on the
403 role of cooperators: they produce costly virulence factors that are then shared with and
404 exploited by the susceptible cells [27,59,60]. This scenario could apply to tobramycin-

405 gallium/furanone combinations, where resistant clones had mutations in *fusA1* known
406 to be associated with the restoration of protein synthesis [48]. Similar social effects
407 could explain selection abrogation in the case of meropenem-gallium combination.
408 Here, the meropenem resistant clone has a mutation in *mpl*, which can trigger the
409 overexpression of the β-lactamase *ampC* resistance mechanism [43]. Since β-
410 lactamase enzyme secretion and extracellular antibiotic degradation is itself a
411 cooperative behaviour [61], it could together with the virulence factor sharing described
412 above compromise the spread of the resistant clone. Clearly, all these explanations
413 remain speculative and further studies are required to understand the molecular and
414 evolutionary basis of abrogated and reversed selection for resistance.
415
416 In summary, drug combination therapies are gaining increased attention as more
417 sustainable strategies to treat infections, limiting the spread of antibiotic resistance
418 [62–65]. They are already applied to a number of diseases, including cancer [66], HIV
419 [67] and tuberculosis infections [68]. Here we probed the efficacy and evolutionary
420 robustness of antibiotics combined with anti-virulence compounds. This is an
421 interesting combination because antibiotic treatments alone face the problem of rapid
422 resistance evolution, whereas antivirulence drugs are evolutionarily more robust but
423 can only disarm and not eliminate pathogens. Combinatorial treatments seem to bring
424 the strengths of the two approaches together: efficient removal of bacteria by the
425 antibiotics combined with disarming and increased evolutionary robustness of the
426 antivirulence compounds. While our findings are promising and could set the stage for
427 a novel class of combinatorial treatments, there are still many steps to take to bring
428 our approach to the clinics. First, it would be important to quantify the rate of resistance
429 evolution directly under the combinatorial treatments to test whether drug combination

430 itself slows down resistance evolution [62]. The level of evolutionary robustness of the
431 antivirulence compound would be of particular importance here, as it is known to vary
432 across compounds [27,38]. For example, previous studies showed that resistance to
433 furanone can arise relatively easily [57] while gallium seems to be more evolutionarily
434 robust [38]. Second, the various antibiotic-antivirulence combinations must be tested
435 in relevant animal host models, as host conditions including the increased spatial
436 structure inside the body can affect the competitive dynamics between strains,
437 potentially influencing the outcome of the therapy [69,70]. Relevant in this context
438 would also be tests that closely examine the toxicity of the antivirulence compounds
439 for mammalian cells, an aspect that has received little attention so far [17,71]. Third,
440 our findings suggest that the beneficial effects of combination therapy depend on the
441 specific antibiotic resistance mechanism involved. This hypothesis should be tested in
442 more detail by using sets of mutants that are resistant to the same antibiotic but through
443 different mechanisms. Finally, the observed patterns of drug synergy and reversed
444 selection for resistance are concentration dependent (Fig 4-5). Thus, detailed research
445 on drug delivery and the pharmacodynamics and pharmacokinetics of combination
446 therapies would be required [56], especially to determine the drug interaction patterns
447 within patients.

448 ## Materials and methods

449 ### Bacterial strains

450 For all our experiments, we used *P. aeruginosa* PAO1 (ATCC 15692). In addition to
451 the wildtype PAO1, we further used two isogenic variants tagged with either a
452 constitutively expressed GFP or mCherry fluorescent protein. Both fluorescently
453 tagged strains were directly obtained from the wildtype PAO1 using the miniTn7-
454 system to chromosomally integrate a single stable copy of the marker gene, under the
455 strong constitutive Ptac promoter, at the *att*Tn7 site [72]. The gentamycin resistance
456 cassette, required to select for transformed clones, was subsequently removed using
457 the pFLP2-encoded recombinase [72]. Antibiotic resistant clones used for competition
458 assays were generated through experimental evolution and are listed in Table 1
459 together with their respective mutations.

460

461 ### Media and growth conditions

462 For all experiments, overnight cultures were grown in 8 ml Lysogeny broth (LB, Sigma
463 Aldrich, Switzerland) in 50 ml Falcon tubes, incubated at 37°C, 220 rpm for 18 hours.
464 We washed overnight cultures with 0.8% NaCl solution and adjusted them to OD_{600} =
465 1 (optical density at 600 nm). Bacteria were further diluted to a final starting OD_{600} =
466 10^{-3} for all experiments. We used two different media, where the targeted virulence
467 factors (pyoverdine or protease) are important. For pyoverdine, we used iron-limited
468 CAA (CAA+Tf) [0.5% casamino acids, 5 mM $K_2HPO_4 \cdot 3H_2O$, 1 mM $MgSO_4 \cdot 7H_2O$],
469 buffered at neutral pH with 25 mM HEPES buffer and supplemented with 100 µg/ml
470 human apo-transferrin to chelate iron and 20 mM $NaHCO_3$ as a co-factor. As an iron-
471 rich control medium, we used CAA supplemented with 25 mM HEPES and 20 µM

472 $FeCl_3$, but without apo-transferrin and 20 mM $NaHCO_3$ to create conditions that do not
473 require pyoverdine for growth [36].
474
475 For QS-regulated proteases, we used casein medium (CAS) [0.5% casein, 5 mM
476 $K_2HPO_4 \cdot 3H_2O$, 1 mM $MgSO_4 \cdot 7H_2O$], supplemented with 25 mM HEPES buffer and
477 0.05% CAA. In this medium, proteases are required to digest the casein. A small
478 amount of CAA was added to allow cultures to have a growth kick start prior to protease
479 secretion [73]. As a control, we used CAA supplemented with 25 mM HEPES buffer, a
480 medium in which proteases are not required. All chemicals were purchased from
481 Sigma Aldrich, Switzerland. The CAS medium is intrinsically turbid due to the poor
482 solubility of casein, which can interfere with the growth kinetics measured via optical
483 density (S7A Fig). To solve this issue, we used mCherry fluorescence intensity as a
484 reliable proxy for growth in CAS (S7B-C Fig).
485
486 **Single drug growth and virulence factor inhibition curves**
487 To determine the activity range of each antibiotic (ciprofloxacin, colistin, meropenem,
488 tobramycin) and antivirulence drug (gallium as $GaNO_3$ and furanone C-30), we
489 subjected PAO1 bacterial cultures to two different 7-step serial dilutions for each
490 antibacterial. Ciprofloxacin: 0-4 µg/ml; colistin: 0-0.4 µg/ml in CAA+Tf and 0-20 µg/ml
491 in CAS; meropenem: 0-14 µg/ml; tobramycin: 0-8 µg/ml; gallium: 0-200 µM; furanone
492 C-30: 0-390 µM. All antibacterials were purchased from Sigma Aldrich, Switzerland.
493 Overnight cultures were prepared and diluted as explained above and then added into
494 200 µl of media on 96-well plates with six replicates for each drug concentration. Plates
495 were incubated statically at 37°C and growth was measured either as OD_{600} (in
496 CAA+Tf) or mCherry fluorescence (excitation 582 nm, emission 620 nm in CAS) after

497 48 hours using a Tecan Infinite M-200 plate reader (Tecan Group Ltd., Switzerland).
498 Control experiments (S8 Fig) confirmed that endpoint OD_{600} or mCherry
499 measurements showed strong linear correlations ($0.858 < R^2 < 0.987$) with the growth
500 integral (area under the growth curve), which is a good descriptor of the overall
501 inhibitory effects covering the entire growth period [74].
502
503 At this time point, we further quantified pyoverdine production through its natural
504 fluorescence (excitation 400 nm, emission 460 nm, a readout that scales linearly with
505 pyoverdine concentration in the medium) and protease production in the cell-free
506 supernatant using the protease azocasein assay (adapted from [38] shortening
507 incubation time to 30 min). The two metals, gallium and bromine (in Furanone C-30),
508 alter the fluorescence levels of pyoverdine and mCherry in a concentration dependent
509 manner. To account for this effect, we established calibration curves and corrected all
510 fluorescence measures accordingly (as described in S9 Fig).
511
512 **Antibiotic-antivirulence combination assays**
513 From the single drug dose-response curves, we chose for each drug nine
514 concentrations (including no drugs) to cover the entire activity range in each medium
515 including no, intermediate and strong inhibitory growth effects on PAO1. (S2 Table).
516 We then combined these drug concentrations in a 9x9 matrix for each of the eight
517 antibiotic-antivirulence pairs, and repeated the growth experiment for all combinations
518 in six-fold replication, exactly as described above. After 48 hours of incubation, we

519 measured growth and virulence factor production following the protocols described
520 above.
521
522 **Synergy degree of drug-combinations**
523 We used the Bliss independence model to calculate the degree of synergy (*S*), for both
524 growth and virulence factor inhibition, for each of the antibiotic-antivirulence
525 combinations [75–77]. The Bliss model has been suggested as the best model of
526 choice for drugs with different modes of actions and targets [76], as it is the case for
527 antibiotics and antivirulence compounds. We used the formula $S = f_{X,0} \cdot f_{0,Y} - f_{X,Y}$,
528 where $f_{X,0}$ is the growth (or virulence factor production) level measured under antibiotic
529 exposure at concentration X; $f_{0,Y}$ is the growth (or virulence factor production) level
530 measured under antivirulence exposure at concentration Y; and $f_{X,Y}$ is the growth (or
531 virulence factor production) level measured under the combinatorial treatment at
532 concentrations X and Y. If $S = 0$ then the two drugs act independently. Conversely, S
533 < 0 indicates antagonistic drug interactions, while $S > 0$ indicates synergy.
534
535 **Experimental evolution under antibiotic treatment**
536 To select for antibiotic resistant clones, we exposed overnight cultures of PAO1
537 wildtype (initial $OD_{600} = 10^{-4}$) to each of the four antibiotics in LB medium (antibiotic
538 concentrations, ciprofloxacin: 0.15 µg/ml; colistin: 0.5 µg/ml; meropenem: 0.8 µg/ml;
539 tobramycin: 1 µg/ml) in six-fold replication. These antibiotic concentrations initially
540 caused a 70-90% reduction in PAO1 growth compared to untreated cultures,
541 conditions that imposed strong selection for the evolution of resistance. The evolution
542 experiment ran for seven days, whereby we diluted bacterial cultures and transferred
543 them to fresh medium with the respective treatment with a dilution factor of 10^{-4}, every

544 24 hours. At the end of each growth cycle, we measured growth (OD_{600}) of the evolving
545 lineages using a SpectraMax® Plus 384 plate reader (Molecular Devices,
546 Switzerland).
547
548 **Phenotypic and genetic characterization of resistance**
549 Following experimental evolution, we screened the evolved lines for the presence of
550 antibiotic resistant clones. For each antibiotic we plated four evolved lines on LB plates
551 and isolated single clones, which we then exposed in liquid culture to the antibiotic
552 concentration they experienced during experimental evolution. Among those that
553 showed growth restoration (compared to the untreated wildtype), we picked two
554 random clones originating from different lineages per antibiotic for further analysis. We
555 had to adjust our sampling design in two cases. First, only one population survived our
556 ciprofloxacin treatment and thus only one resistant clone could be picked for this
557 antibiotic. Second, clones evolved under colistin treatment grew very poorly in CAS
558 medium and therefore we included an experimentally evolved colistin resistant clone
559 from a previous study, which did not show compromised growth in CAS (see [38] for a
560 description on the experimental evolution). Altogether, we had seven clones (one clone
561 per antibiotic was allocated to one of the two media, except for ciprofloxacin). For all
562 of these clones, we re-established the drug-response curves in either CAA+Tf or CAS
563 and quantified the IC50 values (S4 Fig). For all cases, the IC50 of the AtbR clones was
564 significantly higher than the ones of the antibiotic-sensitive wildtype ($-187.30 \leq t \leq -$
565 3.10, $p < 0.01$ for all AtbR clones; S4 Fig). Furthermore, we examined whether
566 resistance to antibiotics can lead to collateral sensitivity or cross-resistance to
567 antivirulence compounds, and that is why also established the dose-response curves
568 for all the seven AtbR clones for the respective antivirulence compounds. As before,

569 we exposed the clones and the wildtype PAO1 to a range of gallium (0-50 μM) or
570 furanone (0-390 μM) concentrations in CAA+Tf or CAS, respectively, and compared
571 their IC50 values.
572
573 We further isolated the genomic DNA of the selected evolved antibiotic resistant clones
574 and sequenced their genomes. We used the GenElute Bacterial Genomic DNA kit
575 (Sigma Aldrich) for DNA isolation. DNA concentrations were assayed using the
576 Quantifluor dsDNA sample kit (Promega, Switzerland). Samples were sent to the
577 Functional Genomics Center Zurich for library preparation (TruSeq DNA Nano) and
578 sequencing on the Illumina MiSeq platform with v2 reagents and pair-end 150 bp
579 reads. In a first step, we mapped the sequences of our ancestral wildtype PAO1 strain
580 (ENA accession number: ERS1983671) to the *Pseudomonas aeruginosa* PAO1
581 reference genome (NCBI accession number: NC_002516) with snippy
582 (https://github.com/tseemann/snippy) to obtain a list with variants that were already
583 present at the beginning of the experiment. Next, we quality filtered the reads of the
584 evolved clones with trimmomatic [78], mapped them to the reference genome and
585 called variants using snippy. Detected variants were quality filtered and variants
586 present in the ancestor strain were excluded from the dataset using vcftools [79]. The
587 mapping files generated in this study are deposited in the European Nucleotide Archive
588 (ENA) under the study accession number PRJEB32766.
589
590 **Monoculture and competition experiments between sensitive and resistant**
591 **clones**
592 To examine the effects of combination treatments on the growth and the relative fitness
593 of antibiotic resistant clones, we subjected the sensitive wildtype PAO1 (tagged with

594 GFP) and the experimentally evolved antibiotic resistant clones (Table 1), alone or in
595 competition, to six different conditions: (i) no drug treatment; (ii) antibiotics alone; (iii-
596 iv) two concentrations of antivirulence compounds alone and (v-vi) the same two
597 concentrations of antivirulence compounds combined with antibiotics. Antibiotic
598 concentrations are listed in the S2 Table, while antivirulence concentrations were as
599 follows, gallium: 1.56 μM (low), 6.25 μM (intermediate); furanone: 6.3 μM (low), 22.8
600 μM (intermediate). Bacterial overnight cultures were prepared and diluted as described
601 above. Competitions were initiated with a mixture of 90% sensitive wildtype cells and
602 10% resistant clones to mimic a situation where resistance is still relatively rare. Mixes
603 alongside with monocultures of all strains were inoculated in either 200 μl of CAA+Tf
604 or CAS under all the six treatment regimes. We used flow cytometry to assess strain
605 frequency prior and after a 24 hours competition period at 37°C static (S10 Fig).
606 Specifically, bacterial cultures were diluted in 1X phosphate buffer saline (PBS, Gibco,
607 ThermoFisher, Switzerland) and frequencies were measured with a LSRII Fortessa
608 cell analyzer (BD Bioscience, Switzerland. GFP channel, laser: 488 nm, mirror: 505LP,
609 filter: 530/30; side and forward scatter: 200 V threshold; events recorded with CS&T
610 settings) at the Cytometry Facility of the University of Zurich. We recorded 50'000
611 events before competitions and used a high-throughput sampler device (BD
612 Bioscience) to record all events in a 5 μl-volume after competition. Since antibacterials
613 can kill and thereby quench the GFP signal in tagged cells, we quantified dead cells
614 using the propidium iodide (PI) stain (2 μl of 0.5 mg/ml solution) with flow cytometry
615 (for PI fluorescence: laser: 561 nm, mirror: 600LP, filter: 610/20).
616
617 We used the software FlowJo (BD Bioscience) to analyse data from flow cytometry
618 experiments. We followed a three-step gating strategy: (i) we separated bacterial cells

619 from media and noise background by using forward and side scatter values as a proxy
620 for particle size; (ii) within this gate, we then distinguished live from dead cells based
621 on the PI staining; (iii) finally, we separated live cells into either GFP positive and
622 negative populations. Fluorescence thresholds were set using appropriate control
623 samples: isopropanol-killed cells for PI positive staining and untagged-PAO1 cells for
624 GFP-negative fluorescence. We then calculated the relative fitness of the antibiotic
625 resistant clone as $\ln(v) = \ln\{[a_{24}\times(1-a_0)]/[a_0\times(1-a_{24})]\}$, where a_0 and a_{24} are the
626 frequencies of the resistant clone at the beginning and at the end of the competition,
627 respectively [80]. Values of $\ln(v) < 0$ or $\ln(v) > 0$ indicate whether the frequency of
628 antibiotic resistant clones decreased or increased relative to the sensitive PAO1-GFP
629 strain. To check for fitness effects caused by the fluorescent tag, we included a control
630 competition, where we mixed PAO1-GFP with the untagged PAO1 in a 9:1 ratio for all
631 treatment conditions. We noted that high drug concentrations significantly curbed
632 bacterial growth, which reduced the number of events that could be measured with
633 flow cytometry. This growth reduction increased noise relative to the signal, leading to
634 an overestimation of the GFP-negative population in the mix. To correct for this
635 artefact, we established calibration curves for each individual experimental replicate
636 for how the relative fitness of PAO1-untagged varies as a function of cell density in
637 control competitions with PAO1-GFP. Coefficients of the asymptotic functions used for
638 the correction are available together with the raw dataset.
639

640 **Statistical analysis**

641 All statistical analyses were performed with RStudio v. 3.3.0 [81]. We fitted individual
642 dose response curves with either log-logistic or Weibull functions, and estimated and
643 compared IC50 values using the drc package [82], while dose response curves under

644 combination treatment were fitted using spline functions. We used Pearson correlation
645 coefficients to test for significant associations between the degree of synergy in growth
646 and virulence factor inhibition. We used one-sample t-tests to compare the degree of
647 synergy of each combination of concentrations represented in Fig 4 to zero. We used
648 Welch's two-sample t-test to compare growth between the sensitive wildtype PAO1
649 and the resistant clones under antibiotic treatment. To compare the relative fitness of
650 resistant clones to the reference zero line, we used one-sample t-tests. Finally, we
651 used analysis of variance (ANOVA) to test whether the addition of antivirulence
652 compounds to antibiotics affected the relative fitness of AtbR clones, and whether the
653 outcome of the competition experiment is associated with the degree of synergy of the
654 drug combinations. Where necessary, p-values were adjusted for multiple
655 comparisons using the false discovery rate method.

Acknowledgments

We thank Roland Regös and Désirée Bäder for advice on the Bliss model; Alex Hall, Roland Regös and Frank Schreiber for comments on the manuscripts; David Wilson for experimental support; Selina Niggli, Priyanikha Jayakumar and the Flow Cytometry Facility (University of Zurich) for support with flow cytometry experiments; and the Functional Genomics Center Zurich for technical support with the strain sequencing.

Funding

This project has received funding from the Swiss National Science Foundation (grant no. 31003A_182499 to RK) and the European Research Council (ERC) under the European Union's Horizon 2020 research and innovation programme (grant agreement no. 681295 to RK).

Competing Interests

The authors have no competing interests to declare.

671 ## References

672 1. Rossolini GM, Arena F, Pecile P, Pollini S. Update on the antibiotic resistance
673 crisis. Curr Opin Pharmacol. Elsevier Ltd; 2014;18: 56–60.
674 doi:10.1016/j.coph.2014.09.006
675 2. World Health Organization (WHO). Antimicrobial resistance: Global Health
676 Report on Surveillance [Internet]. Bulletin of the World Health Organization.
677 2014. doi:10.1007/s13312-014-0374-3
678 3. O'Neill J. Antimicrobial Resistance: Tackling a crisis for the health and wealth of
679 nations. Review on Antimicrobial Resistance. London; 2014.
680 doi:10.1038/510015a
681 4. Tacconelli E, Carrara E, Savoldi A, Harbarth S, Mendelson M, Monnet DL, et al.
682 Discovery, research, and development of new antibiotics: the WHO priority list
683 of antibiotic-resistant bacteria and tuberculosis. Lancet Infect Dis. Elsevier;
684 2018;18: 318–327. doi:10.1016/S1473-3099(17)30753-3
685 5. Laxminarayan R, Matsoso P, Pant S, Brower C, Rottingen J-A, Klugman K, et
686 al. Access to effective antimicrobials: a worldwide challenge. Lancet. England;
687 2016;387: 168–175. doi:10.1016/S0140-6736(15)00474-2
688 6. Dickey SW, Cheung GYC, Otto M. Different drugs for bad bugs: antivirulence
689 strategies in the age of antibiotic resistance. Nat Rev Drug Discov. 2017;16: 1–
690 15. doi:10.1038/nrd.2017.23
691 7. Brown D. Antibiotic resistance breakers: can repurposed drugs fill the antibiotic
692 discovery void? Nat Rev Drug Discov. 2015;14: 821–832. doi:10.1038/nrd4675
693 8. Allen RC, Popat R, Diggle SP, Brown SP. Targeting virulence: can we make
694 evolution-proof drugs? Nat Rev Microbiol. 2014;12: 300–308.
695 doi:10.1038/nrmicro3232

696 9. Vale PF, Fenton A, Brown SP. Limiting Damage during Infection: Lessons from
697 Infection Tolerance for Novel Therapeutics. PLOS Biol. 2014;12.
698 doi:10.1371/journal.pbio.1001769
699 10. Vale PF, McNally L, Doeschl-Wilson A, King KC, Popat R, Domingo-Sananes
700 MR, et al. Beyond killing. Evol Med Public Heal. 2016;2016: 148–157.
701 doi:10.1093/emph/eow012
702 11. Ternent L, Dyson RJ, Krachler AM, Jabbari S. Bacterial fitness shapes the
703 population dynamics of antibiotic-resistant and -susceptible bacteria in a model
704 of combined antibiotic and anti-virulence treatment. J Theor Biol. Elsevier;
705 2015;372: 1–11. doi:10.1016/j.jtbi.2015.02.011
706 12. Hentzer M, Wu H, Andersen JB, Riedel K, Rasmussen TB, Bagge N, et al.
707 Attenuation of Pseudomonas aeruginosa virulence by quorum sensing inhibitors.
708 EMBO J. 2003;22: 3803–3815. doi:10.1093/emboj/cdg366
709 13. Banin E, Lozinski A, Brady KM, Berenshtein E, Butterfield PW, Moshe M, et al.
710 The potential of desferrioxamine-gallium as an anti-*Pseudomonas* therapeutic
711 agent. Proc Natl Acad Sci U S A. 2008;105: 16761–16766.
712 doi:10.1073/pnas.0808608105
713 14. Zeng Z, Qian L, Cao L, Tan H, Huang Y, Xue X, et al. Virtual screening for novel
714 quorum sensing inhibitors to eradicate biofilm formation of Pseudomonas
715 aeruginosa. Appl Microbiol Biotechnol. 2008;79: 119–126. doi:10.1007/s00253-
716 008-1406-5
717 15. Jakobsen TH, Van Gennip M, Phipps RK, Shanmugham MS, Christensen LD,
718 Alhede M, et al. Ajoene, a sulfur-rich molecule from garlic, inhibits genes
719 controlled by quorum sensing. Antimicrob Agents Chemother. 2012;56: 2314–
720 2325. doi:10.1128/AAC.05919-11

721 16. Michaud G, Visini R, Bergmann M, Salerno G, Bosco R, Gillon E, et al.
722 Overcoming antibiotic resistance in Pseudomonas aeruginosa biofilms using
723 glycopeptide dendrimers. Chem Sci. 2016;7: 166–182. doi:10.1039/c5sc03635f
724 17. Goss CH, Kaneko Y, Khuu L, Anderson GD, Ravishankar S, Aitken ML, et al.
725 Gallium disrupts bacterial iron metabolism and has therapeutic effects in mice
726 and humans with lung infections. Sci Transl Med. 2018;10: eaat7520.
727 18. Kirienko DR, Kang D, Kirienko N V. Novel Pyoverdine Inhibitors Mitigate
728 Pseudomonas aeruginosa Pathogenesis. Front Microbiol. 2019;9: 3317.
729 19. Breidenstein EBM, de la Fuente-Núñez C, Hancock REW. *Pseudomonas*
730 *aeruginosa*: all roads lead to resistance. Trends Microbiol. 2011;19: 419–426.
731 doi:10.1016/j.tim.2011.04.005
732 20. Gellatly SL, Hancock REW. Pseudomonas aeruginosa: New insights into
733 pathogenesis and host defenses. Pathog Dis. 2013;67: 159–173.
734 doi:10.1111/2049-632X.12033
735 21. Rezzoagli C, Granato ET, Kümmerli R. Harnessing bacterial interactions to
736 manage infections: A review on the opportunistic pathogen Pseudomonas
737 aeruginosa as a case example. J Med Microbiol. 2020;69: 147–161.
738 doi:10.1099/jmm.0.001134
739 22. Hentzer M, Riedel K, Rasmussen TB, Heydorn A, Andersen JB, Parsek MR, et
740 al. Inhibition of quorum sensing in Pseudomonas aeruginosa biofilm bacteria by
741 a halogenated furanone compound Inhibition of quorum sensing in
742 Pseudomonas aeruginosa biofilm bacteria by a halogenated furanone
743 compound. Microbiology. 2002;148: 87–102. doi:10.1099/00221287-148-1-87
744 23. Rasmussen TB, Bjarnsholt T, Skindersoe ME, Hentzer M, Kristoffersen P, Köte
745 M, et al. Screening for Quorum-Sensing Inhibitors (QSI) by Use of a Novel

746 Genetic System, the QSI Selector. J Bacteriol. 2005;187: 1799 LP – 1814.
747 doi:10.1128/JB.187.5.1799-1814.2005
748 24. Defoirdt T. Quorum-Sensing Systems as Targets for Antivirulence Therapy.
749 Trends Microbiol. Elsevier Ltd; 2018;26: 313–328.
750 doi:10.1016/j.tim.2017.10.005
751 25. Kaneko Y, Thoendel M, Olakanmi O, Britigan BE, Singh PK. The transition metal
752 gallium disrupts *Pseudomonas aeruginosa* iron metabolism and has
753 antimicrobial and antibiofilm activity. J Clin Invest. 2007;117: 877–888.
754 doi:10.1172/JCI30783
755 26. Smith DJ, Lamont IL, Anderson GJ, Reid DW. Targeting iron uptake to control
756 *Pseudomonas aeruginosa* infections in cystic fibrosis. Eur Respir J. 2013;42:
757 1723–36. doi:10.1183/09031936.00124012
758 27. Ross-Gillespie A, Weigert M, Brown SP, Kümmerli R. Gallium-mediated
759 siderophore quenching as an evolutionarily robust antibacterial treatment. Evol
760 Med Public Heal. 2014;2014: 18–29. doi:10.1093/emph/eou003
761 28. Imperi F, Massai F, Facchini M, Frangipani E, Visaggio D, Leoni L, et al.
762 Repurposing the antimycotic drug flucytosine for suppression of *Pseudomonas*
763 *aeruginosa* pathogenicity. Proc Natl Acad Sci U S A. 2013;110: 7458–63.
764 doi:10.1073/pnas.1222706110
765 29. DeLeon K, Balldin F, Watters C, Hamood A, Griswold J, Sreedharan S, et al.
766 Gallium Maltolate Treatment Eradicates *Pseudomonas aeruginosa* Infection in
767 Thermally Injured Mice. Antimicrob Agents Chemother. 2009;53: 1331–1337.
768 doi:10.1128/AAC.01330-08
769 30. Kelson AB, Carnevali M, Truong-Le V. Gallium-based anti-infectives: targeting
770 microbial iron-uptake mechanisms. Curr Opin Pharmacol. 2013;13: 707–716.

771 doi:10.1016/j.coph.2013.07.001
772 31. Bonchi C, Imperi F, Minandri F, Visca P, Frangipani E. Repurposing of gallium-
773 based drugs for antibacterial therapy. BioFactors. 2014;40: 303–312.
774 doi:10.1002/biof.1159
775 32. Hijazi S, Visca P, Frangipani E. Gallium-Protoporphyrin IX Inhibits
776 *Pseudomonas aeruginosa* Growth by Targeting Cytochromes. Front Cell Infect
777 Microbiol. 2017;7: 1–15. doi:10.3389/fcimb.2017.00012
778 33. Hijazi S, Visaggio D, Pirolo M, Frangipani E, Bernstein L, Visca P. Antimicrobial
779 activity of gallium compounds on ESKAPE pathogens. Front Cell Infect
780 Microbiol. 2018;8: 316.
781 34. Manny AJ, Kjelleberg S, Kumar N, de Nys R, Read RW, Steinberg P.
782 Reinvestigation of the sulfuric acid-catalysed cyclisation of brominated 2-
783 alkyllevulinic acids to 3-alkyl-5-methylene-2 (5H)-furanones. Tetrahedron.
784 Elsevier; 1997;53: 15813–15826.
785 35. Manefield M, de Nys R, Kumar N, Read R, Givskov M, Steinberg P, et al.
786 Evidence that halogenated furanones from Delisea pulchra inhibit acylated
787 homoserine lactone (AHL)-mediated gene expression by displacing the AHL
788 signal from its receptor protein. Microbiology. 1999;145 (Pt 2: 283–291.
789 36. Kümmerli R, Jiricny N, Clarke LS, West SA, Griffin AS. Phenotypic plasticity of
790 a cooperative behaviour in bacteria. J Evol Biol. 2009;22: 589–598.
791 doi:10.1111/j.1420-9101.2008.01666.x
792 37. Visca P, Imperi F, Lamont IL. Pyoverdine siderophores: from biogenesis to
793 biosignificance. Trends Microbiol. 2007;15: 22–30.
794 doi:10.1016/j.tim.2006.11.004
795 38. Rezzoagli C, Wilson D, Weigert M, Wyder S, Kümmerli R. Probing the

796 evolutionary robustness of two repurposed drugs targeting iron uptake in
797 *Pseudomonas aeruginosa*. Evol Med Public Heal. 2018;1: 246–259.
798 doi:10.1093/emph/eoy026
799 39. Bassetti M, Vena A, Croxatto A, Righi E, Guery B. How to manage
800 Pseudomonas aeruginosa infections. Drugs Context. England; 2018;7: 212527.
801 doi:10.7573/dic.212527
802 40. Rehman A, Patrick WM, Lamont IL. Mechanisms of ciprofloxacin resistance in
803 pseudomonas aeruginosa: New approaches to an old problem. J Med Microbiol.
804 2019;68: 1–10. doi:10.1099/jmm.0.000873
805 41. Poole K, Neshat S, Heinrichs DE, Zhao Q, Tetro K, Bianco N. Expression of the
806 multidrug resistance operon mexA-mexB-oprM in Pseudomonas aeruginosa:
807 mexR encodes a regulator of operon expression. Antimicrob Agents Chemother.
808 2018;40: 2021–2028. doi:10.1128/aac.40.9.2021
809 42. Jochumsen N, Paulander W, Jensen RL, Folkesson A, Molin S, Jelsbak L, et al.
810 The evolution of antimicrobial peptide resistance in Pseudomonas aeruginosa is
811 shaped by strong epistatic interactions. Nat Commun. 2016;7: 13002.
812 doi:10.1038/ncomms13002
813 43. Tsutsumi Y, Tomita H, Tanimoto K. Identification of Novel Genes Responsible
814 for Overexpression of ampC in Pseudomonas aeruginosa PAO1 . Antimicrob
815 Agents Chemother. 2013;57: 5987–5993. doi:10.1128/aac.01291-13
816 44. Muller C, Plésiat P, Jeannot K. A Two-Component Regulatory System
817 Interconnects Resistance to Polymyxins, Aminoglycosides, Fluoroquinolones,
818 and beta-Lactams in Pseudomonas aeruginosa. Antimicrob Agents Chemother.
819 2011;55: 1211–1221. doi:10.1128/AAC.01252-10
820 45. Zhang L, Mah TF. Involvement of a novel efflux system in biofilm-specific

821 resistance to antibiotics. J Bacteriol. 2008;190: 4447–4452.
822 doi:10.1128/JB.01655-07
823 46. Quale J, Bratu S, Gupta J, Landman D. Interplay of efflux system, ampC, and
824 oprD expression in carbapenem resistance of Pseudomonas aeruginosa clinical
825 isolates. Antimicrob Agents Chemother. 2006;50: 1633–1641.
826 doi:10.1128/AAC.50.5.1633-1641.2006
827 47. Pan Y ping, Xu Y hong, Wang Z xin, Fang Y ping, Shen J lu. Overexpression of
828 MexAB-OprM efflux pump in carbapenem-resistant Pseudomonas aeruginosa.
829 Arch Microbiol. Springer Berlin Heidelberg; 2016;198: 565–571.
830 doi:10.1007/s00203-016-1215-7
831 48. Bolard A, Plesiat P, Jeannot K. Mutations in gene fusA1 as a novel mechanism
832 of aminoglycoside resistance. 2017; 33–3. doi:10.1128/AAC.01835-17
833 49. López-Causapé C, Rubio R, Cabot G, Oliver A. Evolution of the *Pseudomonas*
834 *aeruginosa* Aminoglycoside Mutational Resistome In Vitro and in the Cystic
835 Fibrosis Setting. Antimicrob Agents Chemother. 2018;62: e02583-17.
836 doi:10.1128/AAC.02583-17
837 50. Acar JF. Antibiotic synergy and antagonism. Med Clin North Am. 2000;84: 1391–
838 1406. doi:https://doi.org/10.1016/S0025-7125(05)70294-7
839 51. Lehár J, Krueger AS, Avery W, Heilbut AM, Johansen LM, Price ER, et al.
840 Synergistic drug combinations tend to improve therapeutically relevant
841 selectivity. Nat Biotechnol. 2009;27: 659–666. doi:10.1038/nbt.1549
842 52. Alkawash MA, Soothill JS, Schiller NL. Alginate lyase enhances antibiotic killing
843 of mucoid Pseudomonas aeruginosa in biofilms. Apmis. 2006;114: 131–138.
844 doi:10.1111/j.1600-0463.2006.apm_356.x
845 53. Luo J, Dong B, Wang K, Cai S, Liu T, Cheng X, et al. Baicalin inhibits biofilm

846 formation, attenuates the quorum sensing-controlled virulence and enhances
847 Pseudomonas aeruginosa clearance in a mouse peritoneal implant infection
848 model. PLOS One. 2017;12: 1–32.
849 54. Chait R, Craney A, Kishony R. Antibiotic interactions that select against
850 resistance. Nature. 2007;446: 668–671. doi:10.1038/nature05685
851 55. Hegreness M, Shoresh N, Damian D, Hartl D, Kishony R. Accelerated evolution
852 of resistance in multidrug environments. Proc Natl Acad Sci. National Academy
853 of Sciences; 2008;105: 13977–13981. doi:10.1073/PNAS.0805965105
854 56. Baym M, Stone LK, Kishony R. Multidrug evolutionary strategies to reverse
855 antibiotic resistance. Science. 2016;351. doi:10.1126/science.aad3292
856 57. Maeda T, García-Contreras R, Pu M, Sheng L, Garcia LR, Tomás M, et al.
857 Quorum quenching quandary: resistance to antivirulence compounds. ISME J.
858 2012;6: 493–501. doi:10.1038/ismej.2011.122
859 58. Wale N, Sim DG, Jones MJ, Salathe R, Day T, Read AF. Resource limitation
860 prevents the emergence of drug resistance by intensifying within-host
861 competition. Proc Natl Acad Sci. 2017; 201715874.
862 doi:10.1073/pnas.1715874115
863 59. Mellbye B, Schuster M. The sociomicrobiology of antivirulence drug resistance:
864 a proof of concept. MBio. 2011;2: e00131-11. doi:10.1128/mBio.00131-11
865 60. Gerdt JP, Blackwell HE. Competition Studies Confirm Two Major Barriers That
866 Can Preclude the Spread of Resistance to Quorum-Sensing Inhibitors in
867 Bacteria. ACS Chem Biol. 2014;9: 2291–2299. doi:10.1021/cb5004288
868 61. Vega NM, Gore J. Collective antibiotic resistance: Mechanisms and implications.
869 Curr Opin Microbiol. Elsevier Ltd; 2014;21: 28–34.
870 doi:10.1016/j.mib.2014.09.003

871 62. Fischbach MA. Combination therapies for combating antimicrobial resistance.
872 Curr Opin Microbiol. Elsevier Ltd; 2011;14: 519–523.
873 doi:10.1016/j.mib.2011.08.003
874 63. Silver LL. Challenges of Antibacterial Discovery. Clin Microbiol Rev. 2011;24:
875 71–109. doi:10.1128/CMR.00030-10
876 64. Tepekule B, Uecker H, Derungs I, Frenoy A, Bonhoeffer S. Modeling antibiotic
877 treatment in hospitals: A systematic approach shows benefits of combination
878 therapy over cycling, mixing, and mono-drug therapies. PLOS Comput Biol.
879 2017;13: 1–22. doi:10.1371/journal.pcbi.1005745
880 65. Tyers M, Wright GD. Drug combinations: a strategy to extend the life of
881 antibiotics in the 21st century. Nat Rev Microbiol. Springer US; 2019;17: 141–
882 155. doi:10.1038/s41579-018-0141-x
883 66. Bayat Mokhtari R, Homayouni TS, Baluch N, Morgatskaya E, Kumar S, Das B,
884 et al. Combination therapy in combating cancer. Oncotarget. United States;
885 2017;8: 38022–38043. doi:10.18632/oncotarget.16723
886 67. Cihlar T, Fordyce M. Current status and prospects of HIV treatment. Curr Opin
887 Virol. 2016;18: 50–56. doi:https://doi.org/10.1016/j.coviro.2016.03.004
888 68. Ginsberg AM, Spigelman M. Challenges in tuberculosis drug research and
889 development. Nat Med. United States; 2007;13: 290–294. doi:10.1038/nm0307-
890 290
891 69. Zhou L, Slamti L, Nielsen-LeRoux C, Lereclus D, Raymond B. The Social Biology
892 of Quorum Sensing in a Naturalistic Host Pathogen System. Curr Biol. Cell
893 Press; 2014;24: 2417–2422. doi:10.1016/J.CUB.2014.08.049
894 70. Rezzoagli C, Granato E, Kuemmerli R. In vivo microscopy reveals the impact of
895 Pseudomonas aeruginosa social interactions on host colonization. ISME J.

896 2019;
897 71. Proctor CR, McCarron PA, Ternan NG. Furanone quorum-sensing inhibitors with
898 potential as novel therapeutics against Pseudomonas aeruginosa. J Med
899 Microbiol. 2020;69: 195–206. doi:10.1099/jmm.0.001144
900 72. Choi K-H, Schweizer HP. mini-Tn7 insertion in bacteria with single attTn7 sites:
901 example *Pseudomonas aeruginosa*. Nat Protoc. 2006;1: 153–161.
902 doi:10.1038/nprot.2006.24
903 73. Özkaya Ö, Balbontín R, Gordo I, Xavier KB. Cheating on Cheaters Stabilizes
904 Cooperation in *Pseudomonas aeruginosa*. Curr Biol. 2018;26: 2070–2080.
905 doi:10.1016/j.cub.2018.04.093
906 74. Ocampo PS, Lázár V, Papp B, Arnoldini M, Zur Wiesch PA, Busa-Fekete R, et
907 al. Antagonism between bacteriostatic and bactericidal antibiotics is prevalent.
908 Antimicrob Agents Chemother. 2014;58: 4573–4582. doi:10.1128/AAC.02463-
909 14
910 75. Morones-Ramirez JR, Winkler JA, Spina CS, Collins JJ. Silver Enhances
911 Antibiotic Activity Against Gram-Negative Bacteria. Sci Transl Med. 2013;5: 1–
912 12.
913 76. Baeder DY, Yu G, Hozé N, Rolff J, Regoes RR. Antimicrobial combinations: Bliss
914 independence and Loewe additivity derived from mechanistic multi-hit models.
915 Philos Trans R Soc B Biol Sci. 2016;371. Available:
916 http://rstb.royalsocietypublishing.org/content/371/1695/20150294.abstract
917 77. Barbosa C, Beardmore R, Schulenburg H, Jansen G. Antibiotic combination
918 efficacy (ACE) networks for a Pseudomonas aeruginosa model. PLOS Biol.
919 2018;16: 1–25.
920 78. Bolger AM, Lohse M, Usadel B. Trimmomatic: a flexible trimmer for Illumina

921 sequence data. Bioinformatics. 2014;30: 2114–2120.
922 doi:10.1093/bioinformatics/btu170
923 79. Danecek P, Auton A, Abecasis G, Albers CA, Banks E, DePristo MA, et al. The
924 variant call format and VCFtools. Bioinformatics. 2011/06/07. Oxford University
925 Press; 2011;27: 2156–2158. doi:10.1093/bioinformatics/btr330
926 80. Ross-Gillespie A, Gardner A, West SA, Griffin AS. Frequency dependence and
927 cooperation: theory and a test with bacteria. Am Nat. 2007;170: 331–342.
928 doi:10.1086/519860
929 81. R Development Core Team. R: A language and environment for statistical
930 computing. R Foundation for Statistical Computing. Vienna, Austria; 2013.
931 82. Ritz C, Baty F, Streibig JC, Gerhard D. Dose-Response Analysis Using R. PLOS
932 One. 2015;10: 1–13. doi:10.1371/journal.pone.0146021
933 83. Higgins PG, Fluit AC, Milatovic D, Verhoef J, Schmitz FJ. Mutations in GyrA,
934 ParC, MexR and NfxB in clinical isolates of Pseudomonas aeruginosa. Int J
935 Antimicrob Agents. 2003;21: 409–413. doi:10.1016/S0924-8579(03)00009-8
936 84. Miller AK, Brannon MK, Stevens L, Johansen HK, Selgrade SE, Miller SI, et al.
937 PhoQ mutations promote lipid A modification and polymyxin resistance of
938 Pseudomonas aeruginosa found in colistin-treated cystic fibrosis patients.
939 Antimicrob Agents Chemother. 2011;55: 5761–5769. doi:10.1128/AAC.05391-
940 11
941 85. Lee JY, Park YK, Chung ES, Na IY, Ko KS. Evolved resistance to colistin and its
942 loss due to genetic reversion in Pseudomonas aeruginosa. Sci Rep. Nature
943 Publishing Group; 2016;6: 1–13. doi:10.1038/srep25543
944 86. Barrow K, Kwon DH. Alterations in two-component regulatory systems of phoPQ
945 and pmrAB are associated with polymyxin B resistance in clinical isolates of

946 Pseudomonas aeruginosa. Antimicrob Agents Chemother. 2009;53: 5150–
947 5154. doi:10.1128/AAC.00893-09
948 87. Sanz-garcía F, Hernando-amado S, Martínez L. Mutation-Driven Evolution of
949 Pseudomonas aeruginosa in the Presence of either Ceftazidime or Ceftazidime-
950 Avibactam. Antimicrob Agents Chemother. 2018;62: e01379-18.
951 88. Winsor GL, Griffiths EJ, Lo R, Dhillon BK, Shay JA, Brinkman FSL. Enhanced
952 annotations and features for comparing thousands of Pseudomonas genomes
953 in the Pseudomonas genome database. Nucleic Acids Res. 2015;44: D646–
954 D653. doi:10.1093/nar/gkv1227
955

Figures legends

Fig 1. Antibiotic dose response curves for *P. aeruginosa* PAO1. We exposed PAO1 to all four antibiotics in two experimental media: CAA+Tf (iron-limited casamino acids medium with transferrin) and CAS (casein medium). Except for meropenem, higher concentrations of antibiotics were required to inhibit PAO1 in CAS compared to CAA+Tf. Dots show means ± standard error across six replicates. All data are scaled relative to the drug-free treatment. Data stem from two independent experiments using different dilution series. The red dots indicate the highest concentration used for the respective experiments, from which 7-serial dilution steps were tested. Curves were fitted with either log-logistic functions (in CAA+Tf) or with three-parameter Weibull functions (in CAS).

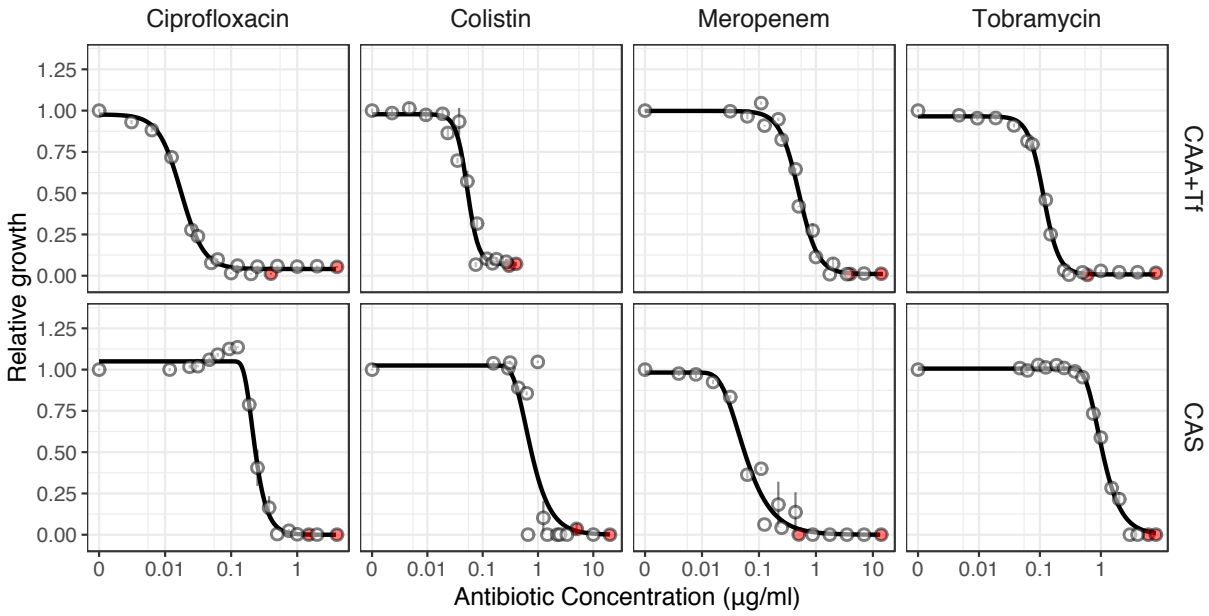

968 **Fig 2. Antivirulence dose response curves for *P. aeruginosa* PAO1 (growth and**
969 **virulence factor production)**. We exposed PAO1 to the antivirulence compounds
970 gallium (inhibiting pyoverdine-mediated iron uptake) and furanone C-30 (blocking
971 quorum sensing response including protease production) both in media where the
972 targeted virulence factors are expressed and required (iron-limited CAA+Tf medium for
973 gallium and CAS medium for furanone) and in control media where the targeted
974 virulence factors are not required (iron-supplemented CAA+Fe medium for gallium and
975 protein digested CAA for furanone). (**A**) Dose-response curves for growth show that
976 both antivirulence compounds reduced bacterial growth, but more so in media where
977 the targeted virulence factor is expressed. This demonstrates that there is a
978 concentration window where the antivirulence compounds have no toxic effects on
979 bacterial cells and just limit growth due to virulence factor quenching. (**B**) Dose-response
980 curves for virulence factor production show that gallium and furanone C-30 effectively
981 inhibit pyoverdine and protease production, respectively, in a concentration-dependent
982 manner. Dots show means ± standard errors across six replicates. All data are scaled
983 relative to the drug-free treatment. Data stem from two independent experiments using
984 different dilution series. The red dots indicate the highest concentration used for the
985 respective experiments, from which 7-serial dilution steps were tested. Curves were
986 fitted with either log-logistic functions (in CAA+Tf) or with three-parameter Weibull
987 functions (in CAS).

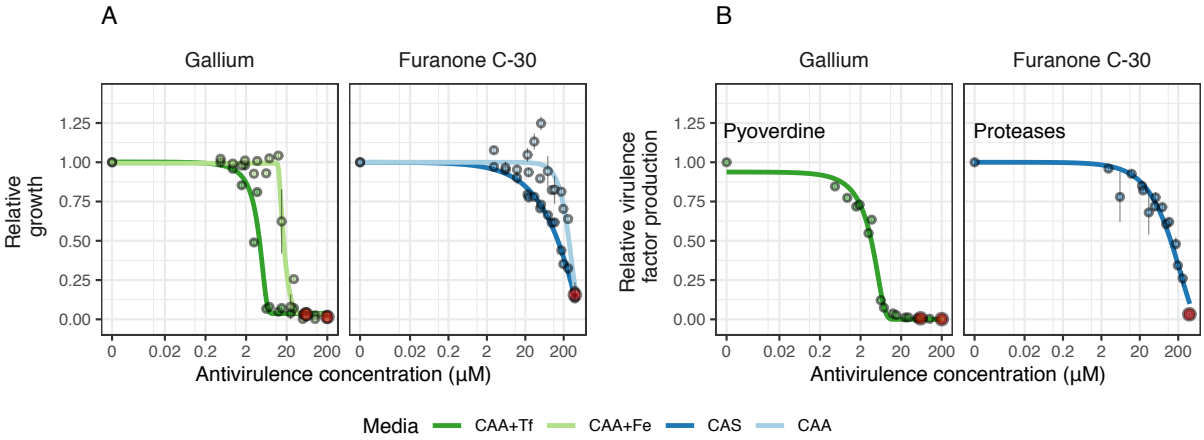

988

989 **Fig 3. Dose response curves for *P. aeruginosa* PAO1 under antibiotic-**
990 **antivirulence combination treatments.** Dose-response curves for growth and
991 virulence factor production for PAO1 were assessed for 9x9 drug concentration matrixes
992 involving the four antibiotics combined with either gallium (**A**) or furanone C-30 (**B**).
993 Experiments were carried out in media where the corresponding virulence factors are
994 required for growth (pyoverdine: CAA+Tf; protease: CAS). Growth and virulence factor
995 production were measured after 48 hours. All values are scaled relative to the untreated
996 control, and data points show the mean across 12 replicates from two independent
997 experiments. We used spline functions to fit the dose-response curves.

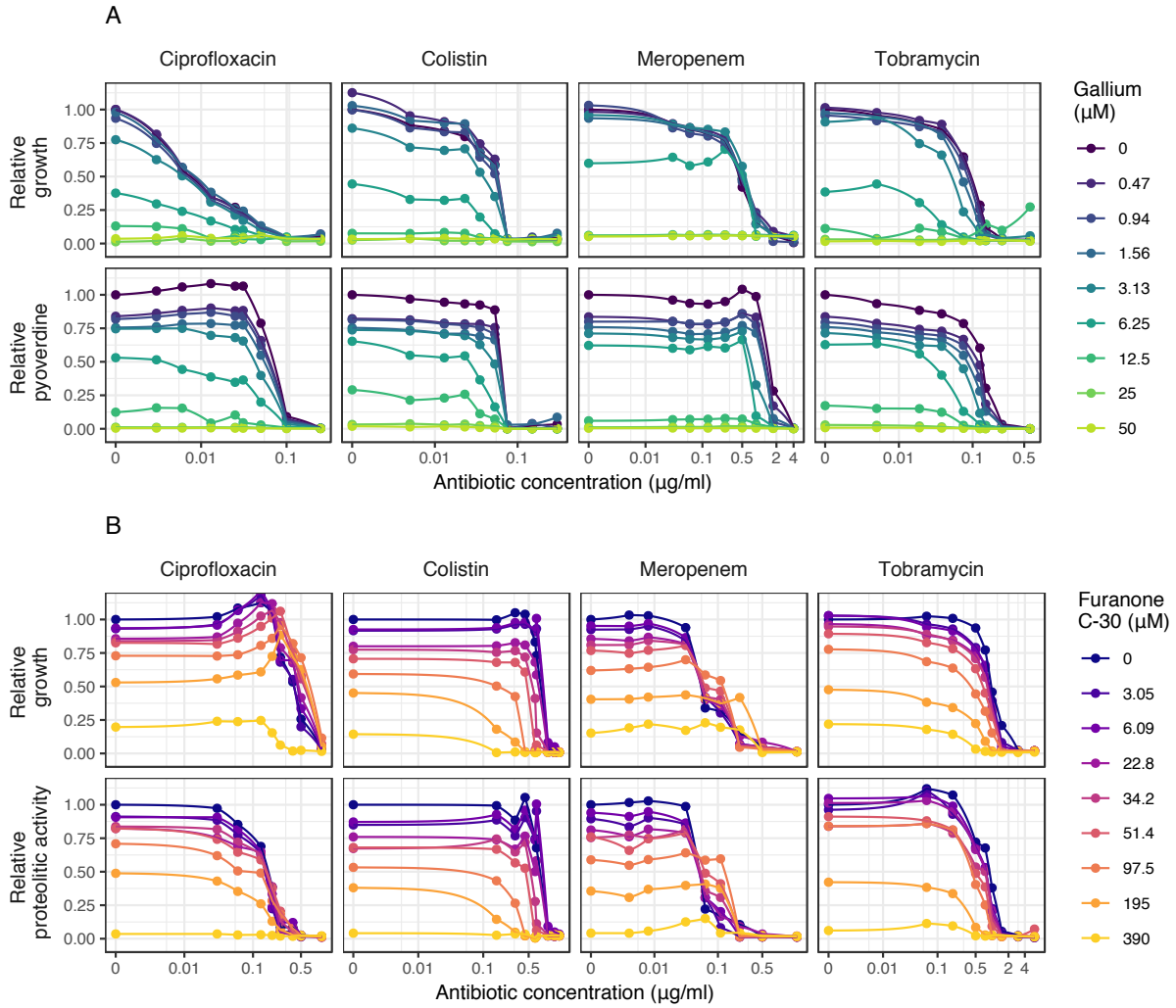

998

999

Fig 4: Drug interaction heatmaps for antibiotic-antivirulence combination treatments. We used the Bliss independence model to calculate the degree of synergy for every single drug combination with regard to growth suppression and virulence factor quenching shown in Fig 3. Heatmaps, depicting variation in drug interactions ranging from antagonism (blue) to synergy (red), are shown for gallium-antibiotic combinations (**A-D** for growth; **E-H** for pyoverdine production) and furanone-antibiotic combinations (**I-L** for growth; **M-P** for protease production). All calculations are based on 12 replicates from two independent experiments.

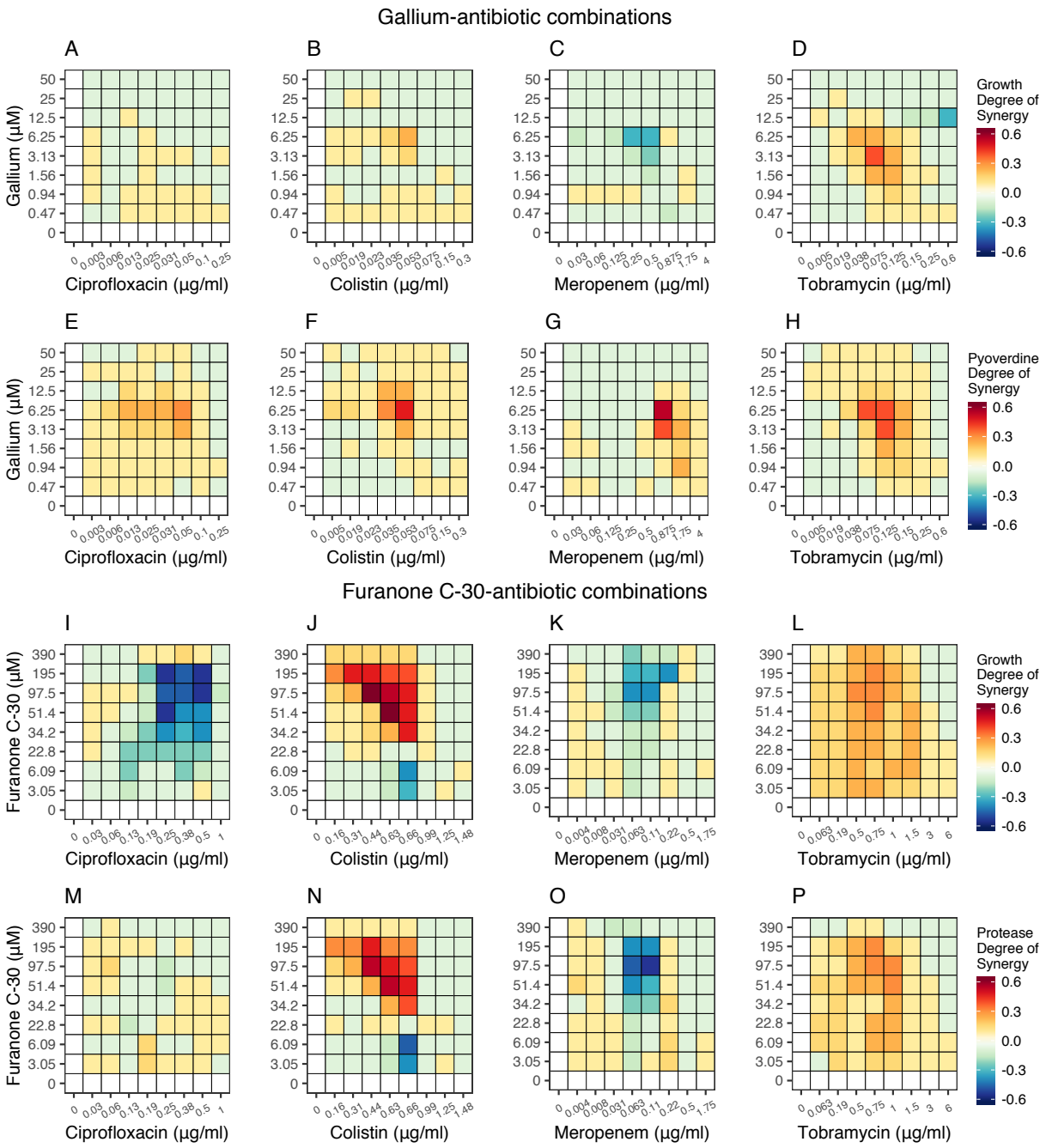

1009 **Fig 5: Effect of combination treatment on growth of antibiotic resistant clones.**
1010 Test of whether the addition of gallium (**A**) or furanone (**B**) can restore growth
1011 suppression in antibiotic resistant clones (AtbR, in orange) relative to the susceptible
1012 wildtype (WT, in black). Under antibiotic treatment and in the absence of antivirulence
1013 compounds, all AtbR strains grew significantly better than the WT (two-sample t-tests, -
1014 26.63 ≤ $t_{21\text{-}40}$ ≤ -3.03, p < 0.01 for all treatment combinations; n.s. = non-significant; * p
1015 <0.05; ** p <0.01; *** p <0.001), a result that holds for both scaled (as shown above)
1016 and absolute growth. In the presence of antivirulence compounds (upper series of
1017 panels without antibiotics (-Atb); lower series of panels with antibiotics (+Atb)), growth
1018 suppression was restored in six out of eight cases. The exceptions were the
1019 ciprofloxacin-furanone and meropenem-furanone combinations. The bottom series of
1020 panels shows the degree of drug synergy for the wildtype and the AtbR clones. All cell
1021 density values (measured with flow cytometry as number of events detected in 5 µl of
1022 culture, after 24 hours) are scaled relative to the untreated control. All data are shown
1023 as means ± standard errors across a minimum of 16 replicates from 4 to 6 independent
1024 experiments.

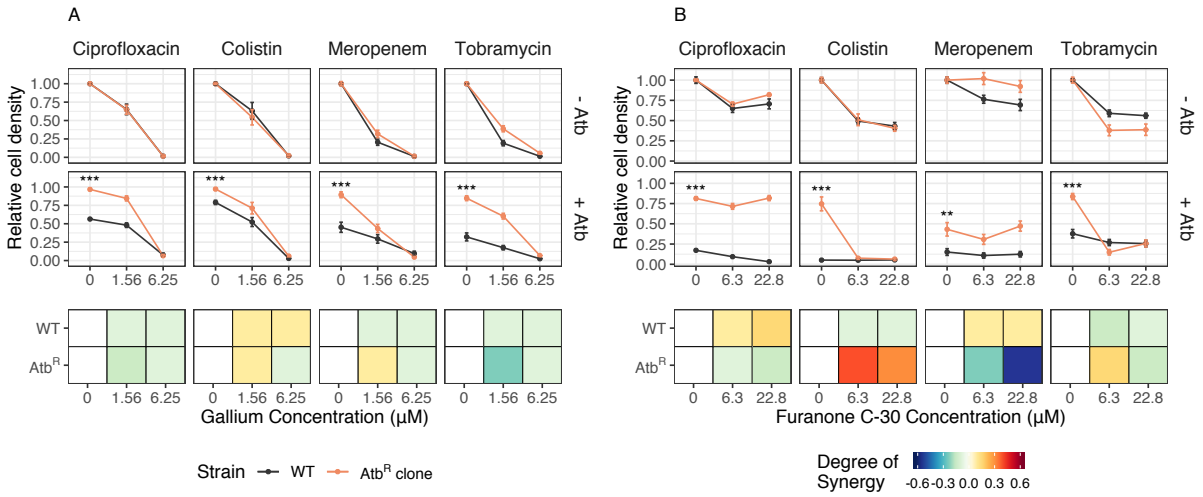

1025

1026 **Fig 6: Effect of combination treatment on the relative fitness of antibiotic resistant**
1027 **clones.** Test of whether antivirulence compounds alone or in combination with
1028 antibiotics can abrogate or revert selection for antibiotic resistance. All AtbR clones were
1029 competed against the susceptible wildtype (WT) for 24 hours, starting at a 1:9 ratio. The
1030 dashed lines denote fitness parity, where none of the competing strains has a fitness
1031 advantage. In the absence of any treatment, all AtbR clones showed a fitness
1032 disadvantage (fitness values < 0) compared to the WT, demonstrating the cost of
1033 resistance. When treated with antivirulence compounds alone, the AtbR clones did not
1034 experience any selective advantage in 14 out of 16 cases (exception: colistin-gallium
1035 combinations). When treated with antibiotics alone, all AtbR clones experienced
1036 significant fitness advantages (fitness values > 0), as expected. When antivirulence
1037 compounds were added as adjuvants to antibiotics, the fitness advantage of AtbR
1038 clones was reduced, abrogated or reversed for six out of eight drug combinations. All
1039 data are shown as means ± standard errors across a minimum of 16 replicates from 4
1040 to 7 independent experiments. Significance levels are based on t-tests or ANOVAs: n.s.
1041 = non-significant; * p <0.05; ** p <0.01; *** p <0.001. See Table S1 for full details on the
1042 statistical analyses.

1043

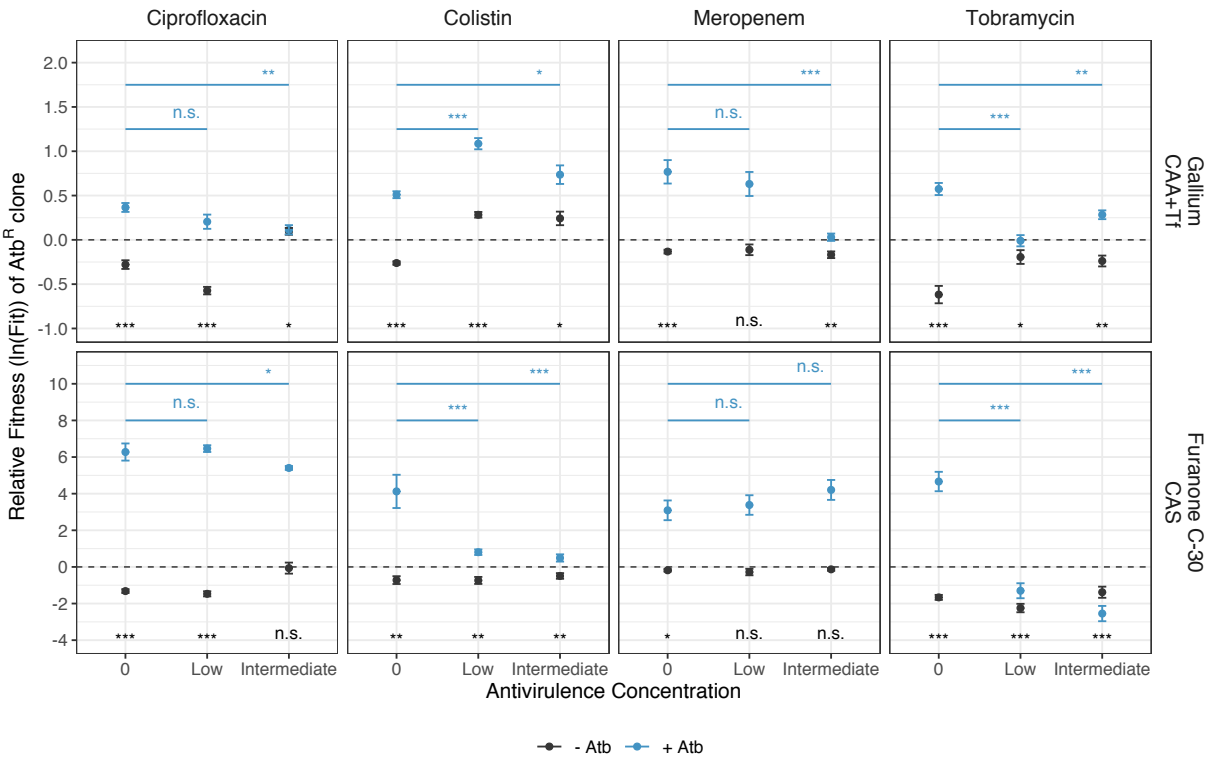

1044

1045 **Table 1. List of mutations in the antibiotic resistant clones**

AtbR clone[a,b]	Combination with	Gene[c]	Description	Mutation type[b]	Reference	Variant	Position[d]	Reference
CpR_1	Gallium Furanone C-30	*gyrB*	DNA gyrase subunit B	INDEL	CCCAGGAG	CG	5671	[40]
		mexR	Multidrug resistance operon repressor	INDEL	ATCAGTGCCT TGTCGCGGCA	AA	471547	[41,83]
CoR_1	Gallium	*phoQ*	Two-component sensor PhoQ	SNP	T	G	1279140	[42,84–86]
CoR_2	Furanone C-30	*phoQ*	Two-component sensor PhoQ	INDEL	T	TC	1279085	[42,84–86]
				SNP	T	C	1279089	
		PA1327	Probable protease	INDEL	CA	C	1440622	
MeR_1	Gallium	*mpl*	UDP-N-acetylmuramate:L-alanyl-gamma-D-glutamyl-meso-diaminopimelate ligase	SNP	T	G	4499740	[43,87]
MeR_2	Furanone C-30	*parR*	Two-component response regulator, ParR	SNP	C	T	1952257	[44]
		PA1874	Hypothetical protein (efflux pump)	COMPLEX	ACCGGG	CCCGTC	2039326	[45]
				SNP	A	G	2039485	
				SNP	C	T	2039494	
				SNP	T	C	2039512	
				SNP	G	A	2039517	
				SNP	T	C	2039524	

				COMPLEX	CGGG	TGGC	2039530	
		nalD	Transcriptional regulator NalD	SNP	A	C	4006981	[46,47]
TbR_1	Gallium	*fusA1*	Elongation factor G	SNP	C	T	4769121	[48]
				SNP	T	G	5253694	
TbR_2	Furanone C-30	*fusA1*	Elongation factor G	SNP	T	C	4770785	[48]
		pscP	Translocation protein in type III secretion system	INDEL	$TG(TTGGCG)_{x11}$	$TG(TTGGCG)_{x12}$	1844903	
		PA4132	Conserved hypothetical protein	SNP	A	C	4621443	

[a]The antibiotic resistant strains are referred to as AtbR throughout the text.

[b]Abbreviations: Atb: antibiotic; Cp: ciprofloxacin; Co: colistin; Me: meropenem; Tb: tobramycin; SNP: single nucleotide polymorphism; INDEL: insertion or deletion; COMPLEX: multiple consecutive SNPs .

[c]Mutations in the ancestor wildtype background compared to the reference PAO1 genome are reported in [38].

[d]Position on PAO1 reference genome [88].